Journal of Chromatography A, 1230 (2012) 100–109

Contents lists available at SciVerse ScienceDirect

Journal of Chromatography A

journal homepage: www.elsevier.com/locate/chroma

Strategy of rearranging the port locations in a three-zone simulated moving bed chromatography for binary separation with linear isotherms

Sungyong Mun*

Department of Chemical Engineering, Hanyang University, Haengdang-dong, Seongdong-gu, Seoul 133-791, South Korea

ARTICLE INFO

Article history:
Received 18 November 2011
Received in revised form 25 January 2012
Accepted 26 January 2012
Available online 4 February 2012

Keywords:
Simulated moving bed chromatography
Binary separation
Port locations
Throughput

ABSTRACT

A three-zone simulated moving bed (SMB) chromatographic process for binary separation, which has been developed previously, was reported to have four ports that are located in the order of desorbent, extract, feed, and raffinate. To make a substantial improvement in the performance of such a three-zone SMB process, the strategy of rearranging the port locations was proposed in this study within a linear isotherm region. The core of the proposed strategy is to transfer the location of the extract port from its classical position (i.e., the position between zones I and II) to the zone III outlet. Simultaneously, the feed and raffinate ports are transferred backwards by one zone. Thus, the order of the proposed port locations follows the order of desorbent, feed, raffinate, and extract. The results from both equilibrium-theory analysis and detailed simulation proved that the proposed strategy was highly effective in improving the product purities or throughput of a three-zone SMB process. Furthermore, it was found that such advantage of the proposed strategy became greater as the difference between the adsorption affinities of the feed components was larger.

1. Introduction

Simulated moving bed (SMB) is a continuous chromatographic separation process with a variety of noteworthy applications in the petrochemical, biochemical, and pharmaceutical industries [1–7]. The major advantage of an SMB chromatographic process is that it proper design can allow the following two states to be maintained simultaneously throughput the SMB operation; (1) continuous loading of the feed into the overlapping region of the two solute bands and (2) continuous collection of the product from the separated region of each solute band. The attainment of such states, which must be a crucial factor in leading to higher productivity and higher purity than conventional batch chromatographic processes [8,9], has been realized in several configurations.

Initially, a classical four-zone SMB configuration has been established for binary or pseudo binary separation of petrochemicals, sugars, and chiral drugs [1–9]. Such a successful application of a classical four-zone configuration was followed by a series of modified or advanced configurations, which included a two-zone SMB [10–12], a three-zone SMB [13–17], a five-zone SMB [18–21], an eight-zone SMB [22], and a nine-zone SMB [23]. The introduction of these SMB configurations proved to be effective in fulfilling additional functions or guaranteeing some process merits that were unattainable by a classical four-zone SMB configuration.

Among the aforementioned SMB configurations, a three-zone SMB is particularly recognized as a good alternative to a classical four-zone SMB, if there is a need for saving the amount of adsorbent due to its expensiveness. Since a three-zone SMB uses one less zone than a four-zone SMB, it will be straightforward to reduce the adsorbent volume of the former to 3/4 of that of the latter while causing little variation in separation performance [13–15]. However, a three-zone SMB inevitably consumes more desorbent because of no recycle of liquid from zone III to zone I [13–15]. Nevertheless, it is certain that a three-zone SMB has sufficient qualifications for one of continuous binary-separation processes, especially in the case where highly expensive adsorbents need to be employed as is often the case with chiral separation task [17].

Fig. 1 shows the schematic diagram of a classical three-zone SMB for binary separation [13–15]. It consists of multiple chromatographic columns, which are partitioned into three zones by the locations of four ports that are arranged in the order of desorbent, extract, feed, and raffinate (Fig. 1). Notice that the feed and extract flow rates result from the difference between the flow rates of the two adjacent zones whereas the desorbent and raffinate flow rates are maintained the same as the flow rates of zones I and III respectively. Under such an arrangement, a counter-current flow between liquid and solid phases is created by moving the ports by one column in the direction of the liquid-phase flow at a predetermined time interval (or switching time). If the flow rates and port switching time are properly designed, most of the lowest-affinity solute molecules can be obtained from the raffinate port

* Tel.: +82 2 2220 0483; fax: +82 2 2298 4101.
E-mail address: munsy@hanyang.ac.kr

0021-9673/$ – see front matter © 2012 Elsevier B.V. All rights reserved.
doi:10.1016/j.chroma.2012.01.081

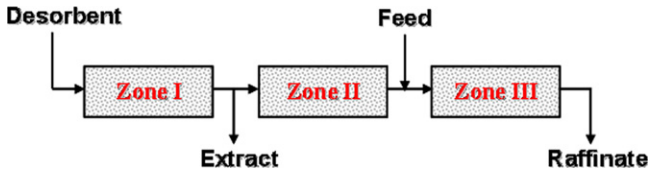

Fig. 1. Schematic diagram of a three-zone SMB based on the classical port locations (or classical three-zone SMB). Switching of ports in the SMB is not shown.

while most of the high-affinity solute molecules can be recovered from the extract port.

To make a substantial improvement in the performance of the aforementioned three-zone SMB process, the strategy of rearranging the port locations is proposed in this study within a linear isotherm region. The key idea of the proposed strategy is to rearrange the four ports in such a way that they can be located in the order of desorbent, feed, raffinate, and extract as shown in Fig. 2. The effect of such a rearrangement of the port locations on the three-zone SMB performance will be investigated first in the frame of equilibrium theory. In addition, the mathematical expressions that can elucidate such effect will be derived mathematically, and they will be further compared between the three-zone SMB based on the proposed port locations and that based on the classical port locations. Then, the merits of the proposed strategy will be validated with detailed simulations, which will be carried out for the three-zone SMB separation of a binary amino acid mixture.

Furthermore, it will be examined how the selectivity between the feed components affect the relative advantages of the proposed port locations over the classical port locations. These tasks will be accompanied by comprehensive optimizations of the three-zone SMBs based on the proposed and the classical port locations, which will be performed by using a highly efficient adaptation of genetic algorithm, NSGA-II-JG (elitist nondominated sorting genetic algorithm with jumping genes) [9]. All the aforementioned works will be carried out for the three-zone SMB with one column per zone.

2. Theory

2.1. Basics and design criteria of a classical three-zone SMB for binary separation

In this section, the basic principle and the design criteria of a classical three-zone SMB process (hereafter, "classical process") are explained. As shown in Fig. 1, the four ports in the classical process are arranged in the order of desorbent, extract, feed, and raffinate ports. Under such a port arrangement, substantial separation between the low-affinity component (A) and the high-affinity component (B) occurs in the two neighboring zones (II and III), which are located in both sides of the feed port and usually called "*separation zones*" [8]. Between these separation zones, zone II plays a role in preventing A from approaching the extract port while zone III plays a role in preventing B from approaching the raffinate port [8]. Based on these two roles, the criteria for linear SMB design have been developed previously [24]. Such two roles can also be

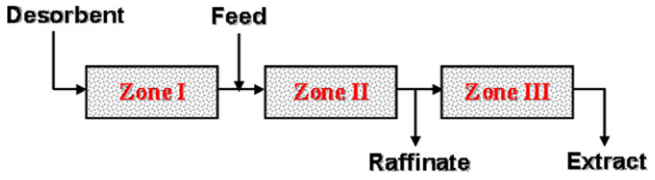

Fig. 2. Schematic diagram of a three-zone SMB based on the proposed port locations (or proposed three-zone SMB). Switching of ports in the SMB is not shown.

expressed in terms of flow-rate-ratios based on equilibrium theory [25] as follows.

$$m^{C}_{S-A} = m^{C}_{2} > H_A \tag{1a}$$

$$m^{C}_{S-B} = m^{C}_{3} < H_B \tag{1b}$$

where the superscript *C* signifies a classical process; the subscripts *A* and *B* indicate the low-affinity and the high-affinity components respectively; and the subscript *S-i* (*i* = *A* or *B*) stands for the separation zone in charge of preventing component *i* from approaching the outlet port for collecting its opponent component. In addition, m_j is the flow-rate-ratio in zone *j*, which is defined as [25]

$$m_j = \frac{Q_j \cdot t_{sw} - V_C \cdot \varepsilon}{V_C \cdot (1-\varepsilon)} \tag{2}$$

where Q_j is the flow rate in zone *j*; t_{sw} is the switching time; V_C is the column volume; and ε is the total porosity. Besides the above flow-rate-ratios in the separation zones (m^{C}_{S-A} and m^{C}_{S-B}), the flow-rate-ratio in the desorbent-loaded zone (m^{C}_{des}) should also satisfy the following constraint for successful separation.

$$m^{C}_{des} = m^{C}_{1} > H_B \tag{3}$$

The role of this constraint is to clear the high-affinity solute molecules (B) from the desorbent-loaded zone (i.e., zone I) within a switching time. To facilitate the application of this constraint in the process design, it is sometime re-expressed into the form of equation by introducing a proper margin factors (or safety factor) as follows.

$$m^{C}_{des} = \beta^{C} H_B \tag{4}$$

where β^C is the margin factor for the desorbent-loaded zone, which must be kept larger than unity for desirable separation.

2.2. Performance of a classical three-zone SMB

The performance of an SMB process is usually evaluated by one of the following three criteria [4,8,9]; (1) throughput, (2) desorbent usage, and (3) product purities. Among these three criteria, throughput and desorbent usage can be represented by feed flow rate and desorbent flow rate respectively.

One of the prevalent ways of investigating the relative superiorities between the performances of two different processes is to compare their feed flow rates (i.e., their throughputs) while keeping the other performance criteria (i.e., desorbent flow rate and product purities) the same between the two processes. On the other hand, if both feed flow rate and desorbent flow rate are kept the same between the two processes, one can compare their product purities for the purpose of determining the better of the two processes.

In case of the classical three-zone SMB (Fig. 1), the feed flow rate that is representative of its throughput can be expressed in terms of the flow-rate-ratios and the margin factor using the relationship of $Q^{C}_{feed} = Q^{C}_{3} - Q^{C}_{2}$ and Eqs. (2) and (4). The resulting expression for the feed flow rate of the classical three-zone SMB is presented below

$$Q^{C}_{feed} = \frac{(m^{C}_{S-B} - m^{C}_{S-A}) \cdot F \cdot Q^{C}_{des}}{\beta^{C} \cdot H_B \cdot F + 1} \tag{5}$$

where $F \equiv (1-\varepsilon)/\varepsilon$ and Q^{C}_{des} is the desorbent flow rate that is representative of the desorbent usage of the SMB process. Note that the feed flow rate is a strong function of the difference between the flow-rate-ratios in the separation zones ($m^{C}_{S-B} - m^{C}_{S-A}$), which has a decisive effect on the product purities as illustrated in the triangle diagram of Fig. 3. As the ($m^{C}_{S-B} - m^{C}_{S-A}$) term decreases, the operating point of the corresponding SMB becomes closer to the diagonal line (Fig. 3), which allows the SMB process to become more robust and thus to achieve higher product purities.

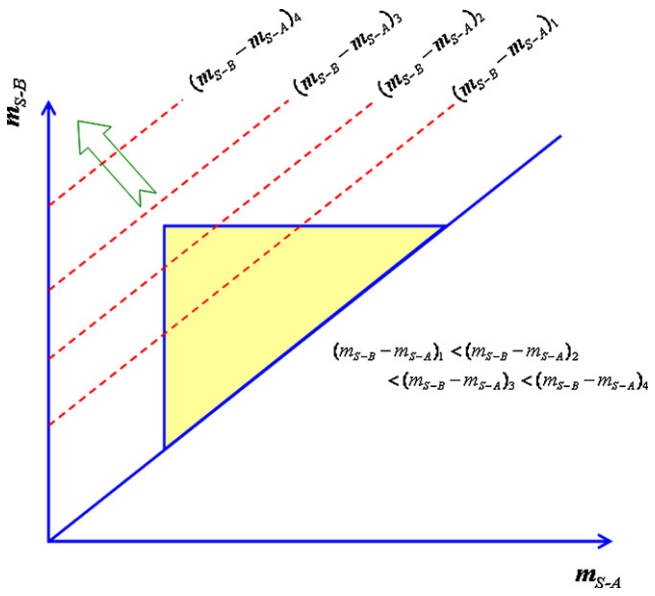

Fig. 3. Illustration of the relationship between the magnitude of $(m_{S-B} - m_{S-A})$ and the distance from the corresponding operating point to the diagonal line in the triangle diagram. m_{S-A}: flow-rate-ratio in the separation zone in charge of preventing component A from approaching the extract port. m_{S-B}: flow-rate-ratio in the separation zone in charge of preventing component B from approaching the raffinate port.

2.3. Principle and design criteria of the proposed three-zone SMB based on the rearrangement of port locations

As a means of improving the performance of a three-zone SMB process, the strategy of rearranging the port locations is proposed in this article. The core of this strategy is to transfer the location of the extract port from its classical position (i.e., the position between zones I and II) to the zone III outlet. Simultaneously, the feed and raffinate ports are transferred backwards by one zone (Fig. 2). Therefore, in the proposed three-zone SMB (hereafter, "proposed process"), the three ports such as extract, feed, raffinate ports are located differently from the classical process. Only the location of the desorbent port is kept the same as in the classical process.

The aforementioned rearrangement of the three ports causes the feed port of the proposed process to be located between zones I and II (Fig. 2), which means that the zones I and II of the proposed process serve as separation zones. Thus, these two zones take the same roles as those of the separation zones (II and III) in the classical process. The design criteria of the proposed process based on such roles of the zones I and II can be expressed as follows.

$$m^{P}_{S-A} = m^{P}_{1} > H_A \tag{6a}$$

$$m^{P}_{S-B} = m^{P}_{2} < H_B \tag{6b}$$

where the superscript *P* stands for the proposed process. In addition to these constraints for the separation zones, it is necessary to clarify how the flow-rate-ratio in the desorbent-loaded zone (m^{P}_{des}) should be constrained for desirable separation. In connection with this issue, it is clear first that m^{P}_{des} should satisfy the same constraint as that of m^{P}_{S-A}, because the desorbent-loaded zone (i.e., zone I) falls on the separation zone *S-A* in case of the proposed process (Fig. 2). Therefore, the first constraint on m^{P}_{des} is given by

$$m^{P}_{des} = m^{P}_{1} > H_A \tag{7}$$

Besides this constraint, an additional constraint on m^{P}_{des} comes from the following two requirements to be satisfied in zone III. The two requirements are that (1) the trailing edge of B should exit zone III within a switching time and (2) the front of A should be confined within zone III during the entire switching time. The feasible range of m^{P}_{3} that can meet such two requirements was derived in Appendix A and the derivation result is presented below.

$$H_B - \frac{\varepsilon}{1-\varepsilon} - m^{P}_{des} < m^{P}_{3} < H_A \tag{8}$$

To guarantee the existence of a feasible m^{P}_{3} value, the upper bound in the above equation should be larger than the lower bound. From this requirement, the additional constraint on m^{P}_{des} can be clarified as follows.

$$m^{P}_{des} > H_B - \left(H_A + \frac{\varepsilon}{1-\varepsilon}\right) \tag{9}$$

This constraint is then combined with the above-mentioned constraint on m^{P}_{des} (Eq. (7)) in order to finalize the constraint on m^{P}_{des} in the following manner.

$$m^{P}_{des} > MAX\left\{H_A, H_B - \left(H_A + \frac{\varepsilon}{1-\varepsilon}\right)\right\} \tag{10}$$

where the *MAX* operator plays a role in generating a larger value between the two values inside the parenthesis. The above constraint on m^{P}_{des} can also be expressed into the following form of equation by employing a proper margin factor (β^{P}).

$$m^{P}_{des} = \beta^{P} \cdot MAX\left\{H_A, H_B - \left(H_A + \frac{\varepsilon}{1-\varepsilon}\right)\right\} \tag{11}$$

where β^{P} is the margin factor for the desorbent-loaded zone, which must be kept larger than unity for desirable separation in the proposed process.

2.4. Performance of the proposed three-zone SMB based on the rearrangement of port locations

In the previous section, the feed flow rate (i.e., throughput) of the classical process was derived in term of the flow-rate-ratios and the margin factor for the desorbent-loaded zone. Following the same procedure, the feed flow rate (i.e., throughput) of the proposed process was derived in this section using the relationship of $Q^{P}_{feed} = Q^{P}_{2} - Q^{P}_{1}$ and Eqs. (2) and (11). The resultant expression for the feed flow rate of the proposed process is presented below

$$Q^{P}_{feed} = \frac{(m^{P}_{S-B} - m^{P}_{S-A}) \cdot F \cdot Q^{P}_{des}}{\beta^{P} \cdot MAX\{H_A, H_B - (H_A + \varepsilon/(1-\varepsilon))\} \cdot F + 1} \tag{12}$$

The above expression for Q^{P}_{feed} (Eq. (12)) can be compared with that for Q^{C}_{feed} (Eq. (5)) in order to clarify which of the two processes has better throughput performance. Recall that in such a comparison, both the desorbent flow rate and the product purities should be kept the same between the two processes, which implies that $Q^{P}_{des} = Q^{C}_{des}$ and $(m^{P}_{S-B} - m^{P}_{S-A}) \approx (m^{C}_{S-B} - m^{C}_{S-A})$ respectively. Under this condition, if there is little difference in the margin factor for the desorbent-loaded zone between the classical and the proposed processes (i.e., $\beta^{P} \approx \beta^{C}$), the relative superiorities of the two processes will be virtually determined by the comparison between H_B and $MAX\{H_A, H_B - (H_A + \varepsilon/(1-\varepsilon))\}$. Since the latter term is definitely smaller than the former, it is certain that the proposed process surpasses the classical process in terms of feed flow rate (or throughput).

In addition to the above comparison of throughput, the product purities that are also an important performance criterion can be compared between the classical and the proposed processes while the feed flow rate and the desorbent flow rate are kept the same between the two processes. If such a comparison is made under a similar margin factor for the desorbent-loaded zone ($\beta^{P} \approx \beta^{C}$), it is evident from Eqs. (5) and (12) that $(m^{P}_{S-B} - m^{P}_{S-A})$ becomes smaller than $(m^{C}_{S-B} - m^{C}_{S-A})$. This indicates that the proposed process can also outperform the classical process in terms of product purities.

In the above comparison based on the mathematical expressions, the margin factor for the desorbent-loaded zone in the proposed process (β^P) was assumed to be similar to that in the classical process (β^C). The use of such assumption is not unreasonable, because it is customary to adopt a moderate value of β ranging from 1.0 to 1.2 for the desorbent-loaded zone (zone I) in the design of SMB processes. In principle, if the β value is chosen to be higher than the one for ensuring the fulfillment of the function in the desorbent-loaded zone (i.e., zone I), a further increase in the β value has no positive effect on the product purities. In particular, if such an increase in the β value is implemented only by increasing the switching time under a fixed Q_{des}, it can rather deteriorate the product purities by hindering the function of the separation zone *S–B*.

Unlike in the above comparative analysis, the assumption of adopting similar margin factors (β) between the two processes will be abandoned in the following comparative work using the model separation system. This is to make more thorough and stricter comparison between the classical and the proposed processes.

2.5. Simulation model

For the simulation and optimization of a multiple chromatographic-column process like the three-zone SMB of our interest, a detailed mathematical model (i.e., chromatographic column model) that can describe accurately the dynamic migration behaviors of solutes through a chromatographic column is needed.

There are several chromatographic column models available in the literature. Among them, the lumped mass-transfer model [3,8,9,26] was chosen as the simulation model of this study because it was reported to be advantageous in the aspects of both accuracy and computation time. This model considers convection, axial dispersion, and mass-transfer between the mobile phase and the solid phase (or adsorbent phase), as presented below.

$$\varepsilon_b \frac{\partial C_{m,i}}{\partial t} + (1-\varepsilon_b)K_{f,i}(C_{m,i} - C_i^*) + u_0\varepsilon_b \frac{\partial C_{m,i}}{\partial z} - \varepsilon_b E_{b,i} \frac{\partial^2 C_{m,i}}{\partial z^2} = 0 \tag{13a}$$

$$\varepsilon_p \frac{\partial C_i^*}{\partial t} + (1-\varepsilon_p)\frac{\partial q_i}{\partial t} = K_{f,i}(C_{m,i} - C_i^*) \tag{13b}$$

where $C_{m,i}$ and C_i^* are the concentration of component i in the mobile phase and that in the pore space of the solid phase respectively; q_i is the solid-phase concentration, which is in equilibrium with C_i^*; u_0 is the liquid interstitial velocity; ε_b and ε_p is the inter-particle and the intra-particle porosities respectively; and E_b is the axial dispersion coefficient. In addition, K_f is the lumped mass-transfer coefficient, which can be estimated from the following equation [3,8,9,26].

$$\frac{1}{K_f} = \frac{(d_p/2)^2}{15\varepsilon_p D_p} + \frac{(d_p/2)}{3k_f} \tag{14}$$

where d_p is the diameter of adsorbent particle; D_p is the intra-particle diffusivity; and k_f is the film mass-transfer coefficient.

The equilibrium relationship between q_i^* and C_i in the above column model equation is usually expressed by an adsorption isotherm model, which is given below in the case of a linear adsorption relationship.

$$q_i^* = H_i C_i \tag{15}$$

where H_i is the Henry constant of component *i*.

To solve the aforementioned model equations, a biased upwind differencing scheme (BUDS) was employed in conjunction with Gear integration having a step size of 0.01. The number of nodes in each column was set at 60. All of these numerical computations were carried out in Aspen Chromatography simulator.

3. Results and discussion

The binary amino acid mixture, which was available in the literature [27], was chosen as a model separation system for investigating the effect of the proposed strategy on product purities and throughput of a three-zone SMB process. In this study, the column configuration of the three-zone SMB was fixed at 1–1–1. The Henry constants and mass-transfer parameters of the two amino acid components comprising the feed mixture were reported in a previous study [27] and they are listed in Table 1 along with the column dimension and the adsorbent particle size. As shown in Table 1, the two components such as phenylalanine and tyrosine have the lower and the higher adsorption-affinities respectively. These components will be denoted as A and B respectively hereafter.

Following the aforementioned binary amino acid mixture, another model separation system with higher selectivity is introduced as a second system for investigating the potential merit of the proposed strategy. In the second system, only the Henry constant of A was decreased from 1.947 to 1.0 while keeping the Henry constant of B the same as that in the first system as shown in Table 1.

3.1. Comparison of product purities between the classical and the proposed three-zone SMB processes

Prior to the comparative analysis of interest in this section, the operating parameters of the classical and the proposed processes were designed to handle the binary separation of the first model system under the conditions of (1) $Q_{feed}^C = Q_{feed}^P = 1.8$ mL/min and (2) $Q_{des}^C = Q_{des}^P = 8$ mL/min. This task was carried out by the following two-step processes: (1) generation of all the possible values for each of the four parameters (Q_1, Q_2, Q_3, t_{sw}) associated with the three-zone SMB operation and (2) search for the operating parameter values leading to high product purities from those generated in the previous step.

In case of the classical process, its design began by calculating t_{sw}^C from Eqs. (2) and (4) at a given margin factor for the desorbent-loaded zone (β^C). In addition, Q_1^C was set at Q_{des}^C while Q_2^C and Q_3^C were allowed to vary under the relationship of $Q_3^C - Q_2^C = Q_{feed}^C$. Thus, the operating parameters of the classical process included a single value for t_{sw}^C, a single value for Q_1^C, and multiple values for each of Q_2^C and Q_3^C at the given β^C value. All of these procedures were then repeated by varying the β^C value.

In case of the proposed process, its design began by calculating t_{sw}^P from Eqs. (2) and (11) at a given margin factor for the desorbent-loaded zone (β^P). In addition, Q_1^C was set at Q_{des}^C, and Q_2^P was determined from the relationship of $Q_2^P - Q_1^P = Q_{feed}^P$. By contrast, Q_3^P was allowed to vary independently of Q_1^P and Q_2^P at the given β^P value. All of these procedures were then repeated by varying the β^P value.

For all the operating parameters generated above, detailed simulations were performed. The simulation results are presented in Fig. 4a for the classical process and in Fig. 4b for the proposed process. Notice that multiple product purities are reported for each β value. This is because each β value is connected with many sets of operating parameters as explained above.

Comparing Fig. 4a and b, one can clearly find that the proposed process surpasses the classical process in obtaining both raffinate product (A) and extract product (B) with high purities. Particularly, it is worth noting that the proposed process can achieve the purities of 98% or higher for both the raffinate and the extract products, which are unattainable in the classical process. To figure out these results more systematically, all the operating parameters associated with Fig. 4a and b were depicted on the plane of (m_{S-A}, m_{S-B}) in Fig. 5, where the m_{S-A} and m_{S-B} of the classical process correspond

Table 1
System parameters and the other details of the binary-separation systems used in the designs, simulations, and optimizations of the classical and the proposed three-zone SMB processes.

		Phenylalanine (A)	Tyrosine (B)
Henry constant (H)	First binary-separation system	1.947	3.229
	Second binary-separation system	1.000	3.229
Molecular diffusivity (D_∞) (cm^2/min)		4.24×10^{-4}	4.12×10^{-4}
Intra-particle diffusivity (D_p) (cm^2/min)		1.02×10^{-4}	1.01×10^{-4}
Axial dispersion coefficient (E_b) (cm^2/min)		Chung and Wen correlation [28]	
Film mass-transfer coefficient (k_f) (cm/min)		Wilson and Geankoplis correlation [29]	
Adsorbent particle diameter (d_p) (μm)		50	
Column length (L_c) (cm)		15	
Column diameter (d_c) (cm)		2	
Inter-particle porosity (ε_b)		0.37	
Intra-particle porosity (ε_p)		0.55	
Feed concentration (C_{feed}) (g/L)		0.3 (for each component)	

Data for H, D_∞, D_p, E_b, k_f, ε_b, and ε_p are from Ref. [27].

to its m_2 and m_3 respectively (i.e., $m^C_{S-A} = m^C_2$ and $m^C_{S-B} = m^C_3$) while the m_{S-A} and m_{S-B} of the proposed process correspond to its m_1 and m_2 respectively (i.e., $m^P_{S-A} = m^P_1$ and $m^P_{S-B} = m^P_2$) as mentioned earlier.

Note in Fig. 5 that the operating points of the classical process move farther away from the vertex of the triangular region as the β^C value increases. Even when the β^C value is set at unity, the operating points are located outside the triangular region. This is why it is impossible for the classical process to achieve successful binary separation under the given feed flow rate ($Q^P_{feed} = 1.8$ mL/min) as seen in Fig. 4a. If the classical process is to guarantee successful separation, its feed flow rate must be reduced to below 1.8 mL/min, which necessarily entails a decrease in throughput.

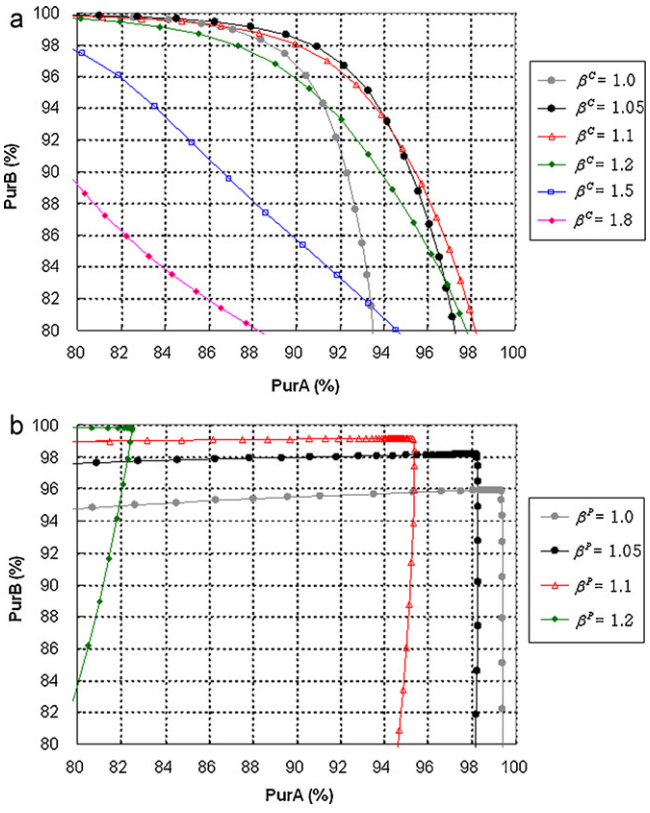

Fig. 4. The product purities of the three-zone SMB from detailed simulations for the first system (lower-selectivity system) in Table 1. The feed flow rate and the desorbent flow rate were fixed at 1.8 mL/min and 8 mL/min respectively. (a) Classical process, (b) Proposed process. PurA and PurB indicate the purities of raffinate and extract products respectively.

By contrast, the proposed process has some operating points that are located inside the triangular region (Fig. 5). It is obvious that such operating points can allow the proposed process to achieve successful separation under the given feed flow rate (β^P = 1.8 mL/min). This can be confirmed from the simulation results for the proposed process based on $Q^C_{feed} = Q^P_{feed} = 1.05$ in Fig. 4b.

In all the above comparative works, the selectivity between phenylalanine (A) and tyrosine (B) was fixed at 1.658. It will be interesting to examine how the selectivity between A and B affects the relative superiority of the proposed process over the classical process in the aspect of product purities. For such an examination, all the above procedures were repeated again for the second model separation system with higher selectivity (Table 1). This task was carried out under the conditions of (1) $Q^C_{feed} = Q^P_{feed} = 4.5$ mL/min and (2) $Q^C_{des} = Q^P_{des} = 8$ mL/min. The reason for adopting higher feed flow rate than in the previous analysis is that higher selectivity usually allows higher feed flow rate.

The results for the aforementioned second system with higher selectivity are presented in Fig. 6. It is clearly seen that the difference of product purities between the classical and the proposed processes is larger in the second model system (Fig. 6) than in the first model system (Fig. 4). This indicates that the relative advantage of the proposed process over the classical process in terms

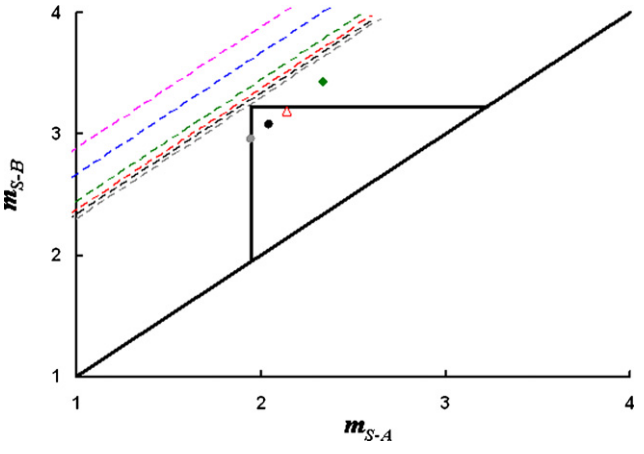

Fig. 5. Comparison between the operating points of the classical and the proposed three-zone SMB processes based on the first system (lower-selectivity system) in Table 1. The feed flow rate and the desorbent flow rate were fixed at 1.8 mL/min and 8 mL/min respectively. Dotted lines indicate the operating points of the classical process, which are based on β^C = 1.0, 1.05, 1.1, 1.2, 1.5, and 1.8 respectively from the lowest position. Symbols indicate the operating points of the proposed process, which are based on β^P = 1.0, 1.05, 1.1, and 1.2 respectively from the left position.

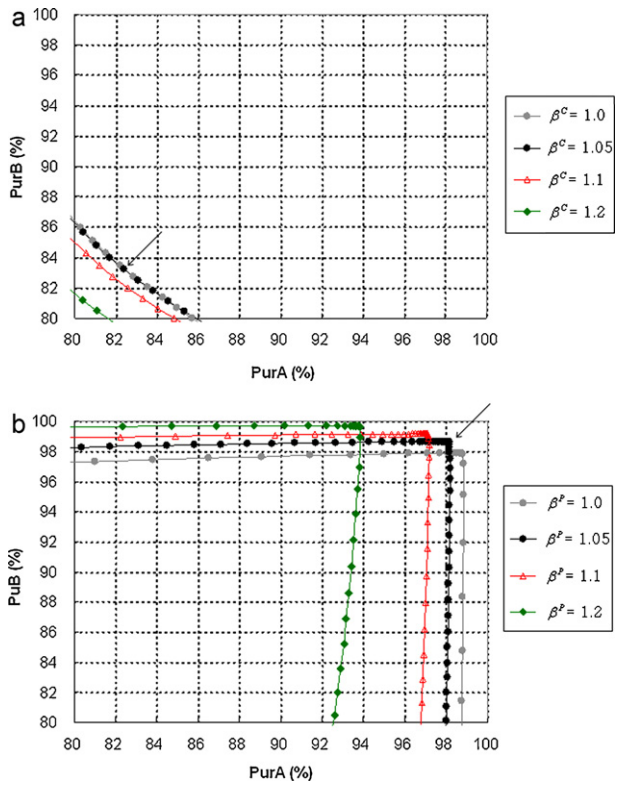

Fig. 6. The product purities of the three-zone SMB from detailed simulations for the second system (higher-selectivity system) in Table 1. The feed flow rate and the desorbent flow rate were fixed at 4.5 mL/min and 8 mL/min respectively. (a) Classical process, (b) Proposed process. PurA and PurB indicate the purities of raffinate and extract products respectively.

of product purities becomes greater as the selectivity increases. Such phenomenon can also be confirmed mathematically using the following equation, which comes from dividing the mathematical expression for Q^P_{feed} (Eq. (12)) by that for Q^C_{feed} (Eq. (5)) and then rearranging the resultant equation.

$$\frac{m^P_{S-B} - m^P_{S-A}}{m^C_{S-B} - m^C_{S-A}} = \left(\frac{Q^P_{feed}}{Q^C_{feed}}\right)\left(\frac{Q^C_{des}}{Q^P_{des}}\right) \times \left(\frac{\beta^P \cdot MAX\{H_A, H_B - (H_A + \varepsilon/(1-\varepsilon))\} \cdot F + 1}{\beta^C \cdot H_B \cdot F + 1}\right) = \left(\frac{Q^P_{feed}}{Q^C_{feed}}\right)\left(\frac{Q^C_{des}}{Q^P_{des}}\right)\left(\frac{\beta^P \cdot H_A \cdot F + 1}{\beta^C \cdot H_B \cdot F + 1}\right) \quad (16)$$

where $MAX\{H_A, H_B - (H_A + \varepsilon/(1-\varepsilon))\}$ in the proposed process is reduced to H_A because the former term inside the parenthesis is always larger than the latter term in the investigated ranges of H_A (=1.0–1.947) and H_B (=3.229).

If there is little difference between the two margin factors (β^P and β^C), the above equation can clearly prove the following two points: (1) $(m^P_{S-B} - m^P_{S-A})$ is always smaller than $(m^C_{S-B} - m^C_{S-A})$ and (2) the magnitude of the difference between $(m^P_{S-B} - m^P_{S-A})$ and $(m^C_{S-B} - m^C_{S-A})$ becomes larger as the H_A value decreases (i.e., the selectivity increases). This implies that an increase in the selectivity widens the distance between the operating points of the classical and the proposed processes in the (m_{S-A}, m_{S-B}) plane, which can readily be confirmed by comparing Figs. 5 and 7. It is thus evident that the extent of the purity improvement resulting from replacement of the classical process by the proposed process is enlarged as the selectivity increases.

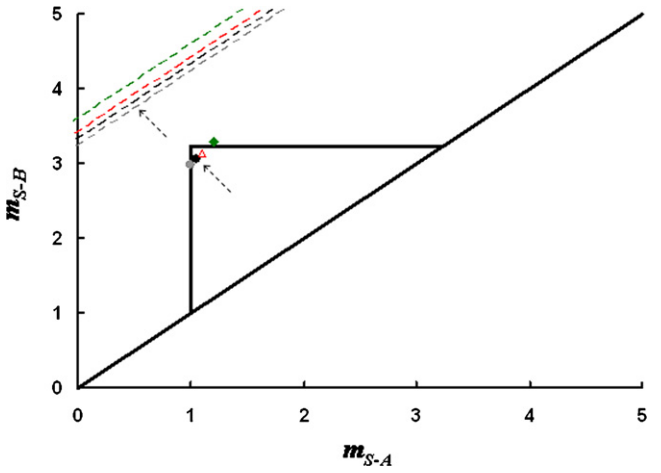

Fig. 7. Comparison between the operating points of the classical and the proposed three-zone SMB processes based on the second system (higher-selectivity system) in Table 1. The feed flow rate and the desorbent flow rate were fixed at 4.5 mL/min and 8 mL/min respectively. Dotted lines indicate the operating points of the classical process, which are based on β^C = 1.0, 1.05, 1.1, and 1.2 respectively from the lowest position. Symbols indicate the operating points of the proposed process, which are based on β^P = 1.0, 1.05, 1.1, and 1.2 respectively from the left position.

3.2. Comparison of column profiles between the classical and the proposed three-zone SMB processes

Using the detailed simulations and the graphical representations of operating points in the (m_{S-A}, m_{S-B}) plane, it was confirmed in the previous section that the proposed process led to higher product purities than the classical process. This point can also be demonstrated by comparing the column profiles of the two processes, which is carried out in this section on the basis of the second model system.

Prior to acquiring the column profiles from the simulations, the operating parameters of the two processes are to be specified in advance. This task was performed by selecting the operating points that were in favor of both the raffinate and the extract purities in Fig. 6. The selected operating points were marked by arrows in Figs. 6 and 7. For these operating points, the simulations were conducted to obtain the column profiles at cyclic steady state for each process.

The resulting column profiles are presented in Fig. 8 for the classical process and in Fig. 9 for the proposed process. Notice that a significant contamination occurs in both the raffinate and the extract ports in case of the classical process (Fig. 8), leading to low purities. To improve the purities of the classical process, there is no choice but to decrease the feed flow rate to below 4.5 mL/min. In contrast, the column profiles of the proposed process clearly demonstrate that the front and the rear of each solute band are well confined within its respective zone (Fig. 9), leading to high purities. This means that the feed flow rate of 4.5 mL/min, which is too high to maintain the purities of about 98% in the classical process, can be handled sufficiently to obtain the purities of 98% or higher in the proposed process.

3.3. Comparison of the classical and the proposed three-zone SMB processes in terms of the optimized throughput under the same purity constraints

In the previous sections, it was confirmed that the proposed process led to better purity performance than the classical process for binary separation. This result suggests that the proposed process can achieve higher throughput (i.e., higher feed flow rate) than the classical process for a given purity specification. To examine

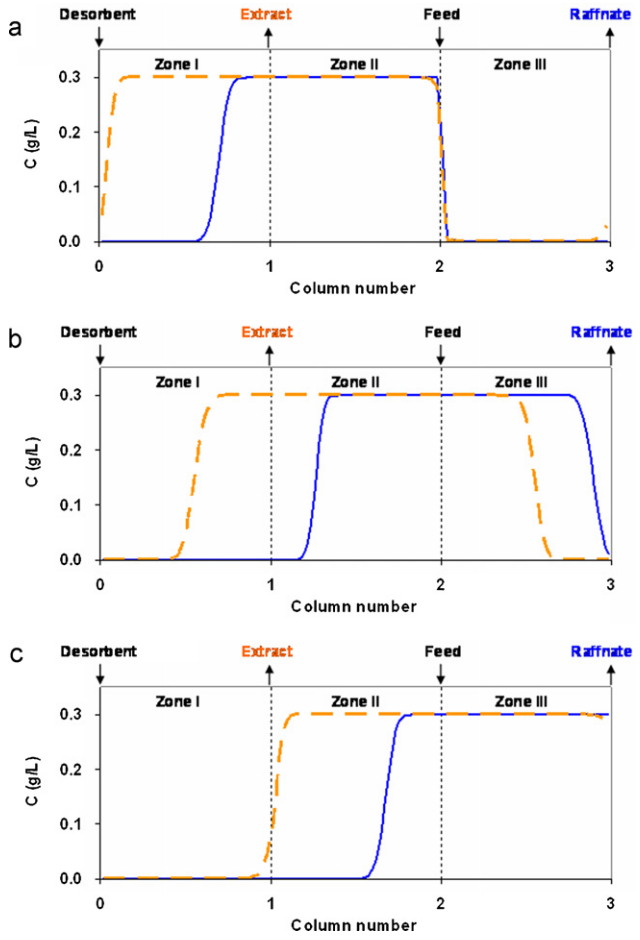

Fig. 8. Steady-state column profiles of the classical process based on the operating point that was selected in favor of both the raffinate and the extract purities in Fig. 6. The selected operating point was marked by arrows in Figs. 6 and 7. (a) At the beginning of a switching period, (b) At the middle of a switching period, (c) At the end of a switching period. The solid and the dotted lines indicate the low-affinity component (A) and the high-affinity component (B) respectively.

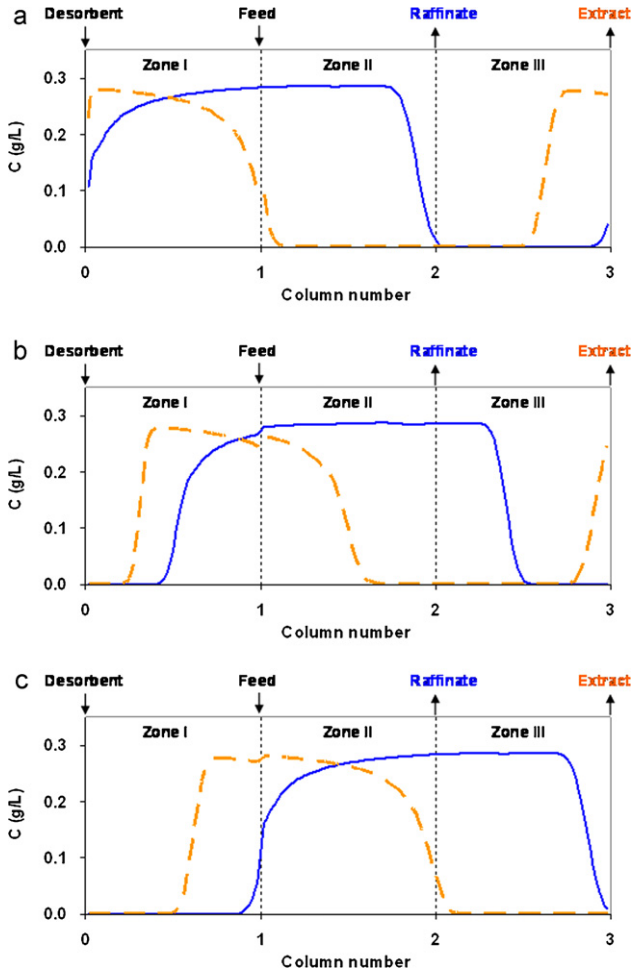

Fig. 9. Steady-state column profiles of the proposed process based on the operating point that was selected in favor of both the raffinate and the extract purities in Fig. 6. The selected operating point was marked by arrows in Figs. 6 and 7. (a) At the beginning of a switching period, (b) At the middle of a switching period, (c) At the end of a switching period. The solid and the dotted lines indicate the low-affinity component (A) and the high-affinity component (B) respectively.

this issue, the classical and the proposed processes were optimized each for maximizing the throughput while the constraints on product purities were kept the same between the two. This task was assisted by the optimization tool of the NSGA-II-JG [9,21,30] coupled with Aspen Chromatography simulator. In this optimization, the feed flow rate was employed as an objective function while the purities of both products were constrained to be higher than 98%. The other details in such an optimization task are presented below. First, those for the classical process are as follows:

$$\text{Max} \quad J = Q^{C}_{\text{feed}}[Q^{C}_{\text{feed}}, Q^{C}_{\text{raf}}, t^{C}_{\text{sw}}] \tag{17a}$$

$$\text{Subject to} \quad \text{PurA} \geq 98\%, \quad \text{PurB} \geq 98\% \tag{17b}$$

$$\text{Fixed variables} \quad Q^{C}_{\text{des}} = 8 \ \text{mL/min} \tag{17c}$$

$$\text{Dependent variables} \quad Q^{C}_{1}(= Q^{C}_{\text{des}}) \tag{17d}$$

$$Q^{C}_{2}(= Q^{C}_{\text{raf}} - Q^{C}_{\text{feed}}) \tag{17e}$$

$$Q^{C}_{3}(= Q^{C}_{\text{raf}}) \tag{17f}$$

$$Q^{C}_{\text{ext}}(= Q^{C}_{\text{des}} + Q^{C}_{\text{feed}} - Q^{C}_{\text{raf}}) \tag{17g}$$

Secondly, the optimization details for the proposed process are as follows:

$$\text{Max} \quad J = Q^{P}_{\text{feed}}[Q^{P}_{\text{feed}}, Q^{P}_{\text{raf}}, t^{P}_{\text{sw}}] \tag{18a}$$

$$\text{Subject to} \quad \text{PurA} \geq 98\%, \quad \text{PurB} \geq 98\% \tag{18b}$$

$$\text{Fixed variables} \quad Q^{P}_{\text{des}} = 8 \ \text{mL/min} \tag{18c}$$

$$\text{Dependent variables} \quad Q^{P}_{1}(= Q^{P}_{\text{des}}) \tag{18d}$$

$$Q^{P}_{2}(= Q^{P}_{\text{des}} + Q^{P}_{\text{feed}}) \tag{18e}$$

$$Q^{P}_{3}(= Q^{P}_{\text{des}} + Q^{P}_{\text{feed}} - Q^{P}_{\text{raf}}) \tag{18f}$$

$$Q^{P}_{\text{ext}}(= Q^{P}_{\text{des}} + Q^{P}_{\text{feed}} - Q^{P}_{\text{raf}}) \tag{18g}$$

where Q_{raf} and Q_{ext} are the flow rates of raffinate and extract streams respectively, and the three flow rates inside the parenthesis (Eqs. (17a) and (18a)) correspond to the decision variables (i.e., the variable to be optimized).

The results from the aforementioned optimization tasks, which were performed on the basis of the system parameters in Table 1, are listed in Table 2. It can readily be seen that the proposed process is capable of handling higher feed flow rate (i.e., higher throughput) than the classical process. Furthermore, it is worth noting that in case of replacing the classical process by the proposed process, the second system with higher selectivity leads to a larger gain in throughput than the first system with lower selectivity.

To make more comprehensive analysis for such effect of selectivity, a series of throughput optimizations were carried out

Table 2
Results from the optimizations of the classical and the proposed three-zone SMB processes for maximizing the feed flow rate (i.e., throughput) under the same purity constraints (≥98%).

	Classical process	Proposed process
The first binary-separation system (H_A = 1.947 and H_B = 3.229)		
Q_{feed} (mL/min)	1.3676	1.8408
PurA (%)	98.0	98.0
PurB (%)	98.0	98.0
Q_{des} (mL/min)	8	8
Q_{ext} (mL/min)	2.1780	7.3583
Q_{raf} (mL/min)	7.1896	2.4825
t_{sw} (min)	10.3042	7.6199
The second binary-separation system (H_A = 1.000 and H_B = 3.229)		
Q_{feed} (mL/min)	2.6667	4.6784
PurA (%)	98.0	98.0
PurB (%)	98.0	98.0
Q_{des} (mL/min)	8	8
Q_{ext} (mL/min)	3.5361	7.3371
Q_{raf} (mL/min)	7.1306	5.3413
t_{sw} (min)	10.4493	5.8983

additionally on the bases of the aforementioned optimization frames (Eqs. (17) and (18)) while changing the A–B selectivity gradually, which was implemented by varying only the Henry constant of A (H_A) from 1.0 to 2.5. The optimization results are presented in Fig. 10. One can see that the throughput increment resulting from the replacement of the classical process by the proposed process becomes markedly larger as the A–B selectivity increases. The major reason for this phenomenon can be explained mathematically using the following equation, which results from dividing the mathematical expression for Q^P_{feed} (Eq. (12)) by that for Q^C_{feed} (Eq. (15)).

$$\frac{Q^P_{feed}}{Q^C_{feed}} = \left(\frac{m^P_{S-B} - m^P_{S-A}}{m^C_{S-B} - m^C_{S-A}}\right)\left(\frac{Q^P_{des}}{Q^C_{des}}\right) \times \left(\frac{\beta^C \cdot H_B \cdot F + 1}{\beta^P \cdot MAX\{H_A, H_B - (H_A + \varepsilon/(1-\varepsilon))\} \cdot F + 1}\right) = \left(\frac{m^P_{S-B} - m^P_{S-A}}{m^C_{S-B} - m^C_{S-A}}\right)\left(\frac{Q^P_{des}}{Q^C_{des}}\right)\left(\frac{\beta^C \cdot H_B \cdot F + 1}{\beta^P \cdot H_A \cdot F + 1}\right) \quad (19)$$

where $MAX\{H_A, H_B - (H_A + \varepsilon/(1-\varepsilon))\}$ in the proposed process is reduced to H_A because the former term inside the parenthesis is always larger than the latter term in the investigated ranges of H_A (=1.0–2.5) and H_B (=3.229). In the above equation, the first two terms on the right-hand side have little effects on Q^P_{feed}/Q^C_{feed} because (1) the same purity constraints were adopted ($(m^P_{S-B} - m^P_{S-A}) \approx (m^C_{S-B} - m^C_{S-A})$) and (2) the same desorbent flow rate ($Q^P_{des} = Q^C_{des}$) was used. Therefore, the magnitude of Q^P_{feed}/Q^C_{feed} is virtually governed by the third term on the right-hand side, particularly by the extent of the difference between H_A and H_B, i.e. the A-B selectivity. It thus becomes clear that as the A-B selectivity increases, the magnitude of Q^P_{feed}/Q^C_{feed} becomes greater, i.e. the relative superiority of the proposed process over the classical process in terms of throughput becomes larger.

In addition to the above comparison of throughput, the product concentration is also worthy to be compared between the classical and the proposed processes because it can affect the efficiency of evaporation process subsequent to the SMB separation step. Such a comparative work was carried out and the results are presented in Fig. 11. Note that the proposed process leads to higher product concentration than the classical process over all the investigated range of selectivity, in which the product concentration was defined as the average of raffinate and extract product concentrations. It is thus evident that the proposed process surpasses the classical process in the aspect of product concentration as well as throughput.

In regard to the aforementioned effect of selectivity on process performance, it is worth adding that an increase in the selectivity leads to an improvement in the performance of a batch chromatography as well as an SMB process. Thus, in the region of extremely high selectivity, the performance of a batch chromatography may sometimes be close to or comparable to that of an SMB process. Nevertheless, it is generally admitted that an SMB process is always superior to a batch chromatography in the aspects of production rate and product concentration. This is mostly due to the fact that the SMB process can obtain high purity and high yield simultaneously while maintaining the partial overlap of two solute bands within the bed, which is however impracticable in the batch chromatography.

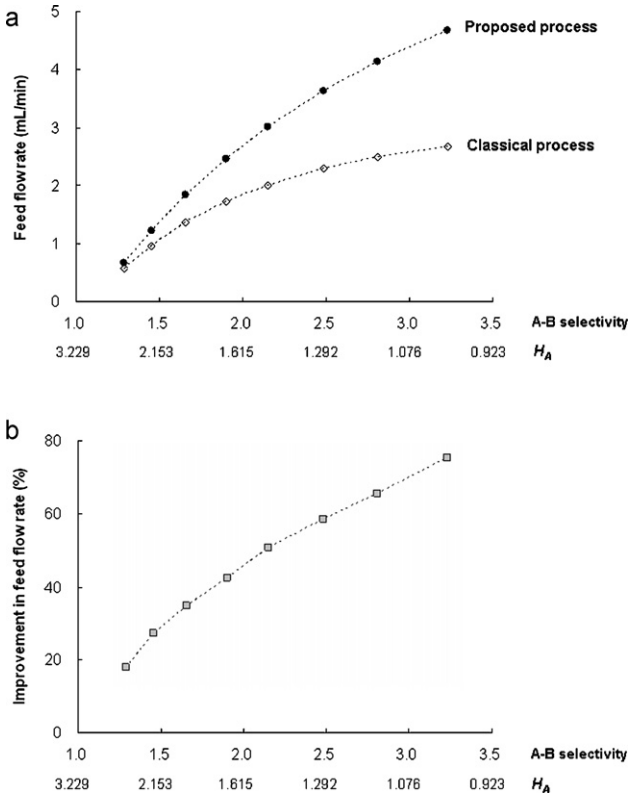

Fig. 10. Effect of the A-B selectivity on the optimized feed flow rate (or optimized throughput) of each three-zone SMB process. (a) Comparison of the optimized feed flow rates of the classical and the proposed processes, (b) Percentage of improvement in the feed flow rate in case of replacing the classical process by the proposed process.

3.4. Effect of the desorbent flow rate on the throughputs of the classical and the proposed three-zone SMB processes

In the above comparison of the optimized throughput (i.e., the optimized feed flow rate) between the two processes, the desorbent flow rate (Q_{des}) was fixed at 8 mL/min. To investigate the effect of Q_{des} on the optimized feed flow rates of the two processes, a series of additional optimization works were carried out in the same way as in the previous section (Eqs. (17) and (18)) while varying only Q_{des} from 4 to 32 mL/min. The results are presented in Fig. 12a for the first system (lower-selectivity system) and in Fig. 12b for the second system (higher-selectivity system).

One can see that the proposed process guarantees higher feed flow rate (i.e., higher throughput) than the classical process over the entire range of Q_{des}. It is also seen that the proposed process consumes less amount of desorbent than the classical process for

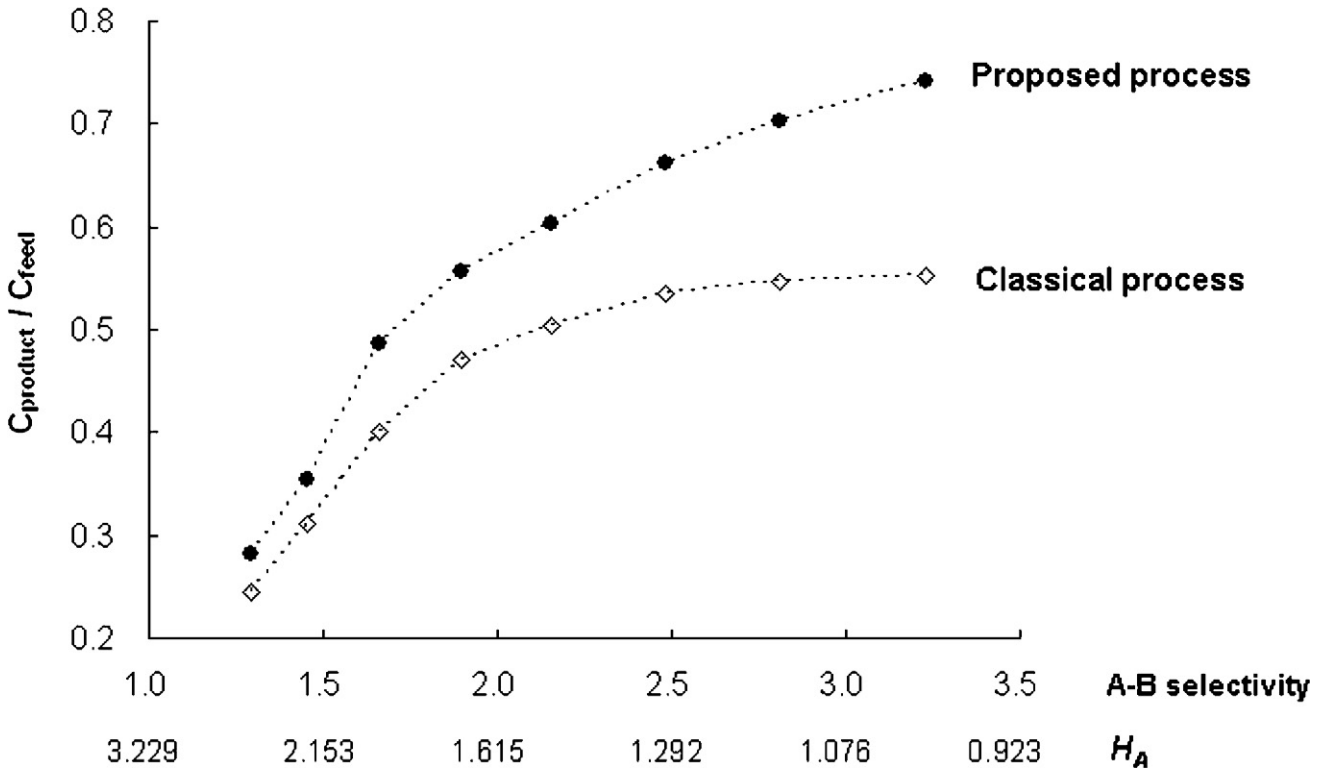

Fig. 11. Comparison of the product concentrations of the classical and the proposed processes while varying the A–B selectivity. The product concentration was defined as the average of raffinate and extract product concentrations.

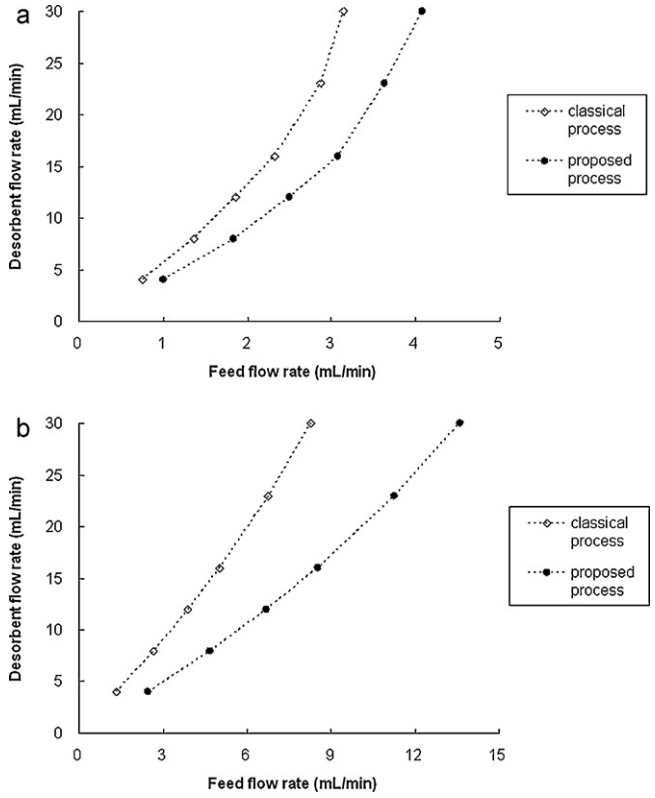

Fig. 12. Comparison of the optimized feed flow rates of the classical and the proposed processes while varying the desorbent flow rate. (a) The first system (lower-selectivity system) in Table 1, (b) The second system (higher-selectivity system) in Table 1.

the same feed flow rate. Furthermore, it can be confirmed from comparison of Fig. 12a and b that the aforementioned merits of the proposed process over the classical process becomes larger as the selectivity increases. The reason for such results can easily be clarified using Eq. (19) and following the same mathematical procedures as in the previous section. So, in this section, a verbal explanation for the reason will be provided instead of the mathematical explanation.

For such an explanation, it is necessary to pay attention to the desorbent-loaded zone (i.e., zone I) of each process. As seen in Figs. 1 and 2, the identity of the component to be desorbed completely from zone I is different between the classical and the proposed processes. Such component is the high-affinity one in case of the classical process, but the low-affinity one in case of the proposed process. This means that the load of desorption in the desorbent-loaded zone is smaller in the proposed process than in the classical process. In addition, the proposed process is in a more advantageous position than the classical process in the aspect of the adsorbent regeneration, which corresponds to the task of removing the high-affinity component from the adsorbent for the purpose of its reuse in the next separation step. The reason is that such an adsorbent-regeneration task is performed in both zones I and III in case of the proposed process whereas it is performed in only zone I in case of the classical process. It is therefore obvious that the load of adsorbent regeneration is smaller in the proposed process than in the classical process.

Due to the aforementioned advantages, the adsorbent utilization in the three zones of the proposed process can be more focused on the increase of throughput (i.e., feed flow rate), compared to the classical process. This can be a major factor in the attainment of higher throughput by the proposed process, and can also be the reason why a larger difference between the adsorption affinities of the feed components leads to a larger gain in the throughput of the proposed process over the classical process.

In all the above comparative works between the proposed and the classical processes, the column configuration was fixed at 1–1–1. It will be a worthwhile task to investigate how the column configuration affects the relative advantage of the proposed process over the classical process. Such a further work is now in progress. The results will be reported in the subsequent paper.

4. Conclusions

In a classical three-zone SMB process, the four ports are located in the order of desorbent, extract, feed, and raffinate. To improve the performance of such a three-zone SMB, the strategy of rearranging the port locations was proposed in this study. The key idea of the proposed strategy was to rearrange the four ports in such a way that they can be located in the order of desorbent, feed, raffinate, and extract. It was found that the three-zone SMB process based on the proposed strategy (or proposed process) surpassed the classical three-zone SMB process (or classical process) in the aspects of product purities and throughput, which was confirmed by both equilibrium-theory analysis and detailed simulations. Furthermore, such a relative merit of the proposed process over the classical process was found to become greater as the selectivity between the feed components was higher. Overall, it is concluded that the proposed port locations are definitely superior to the classical port locations in every respect, as far as a three-zone SMB process is concerned. The strategy proposed in this study is therefore expected to provide a valuable engineering alternative for extending the application scope of a current three-zone SMB process toward the separation tasks demanding a marked improvement in product purities and throughput.

Acknowledgments

This work was supported by the ERC for Advanced Bioseparation Technology, KOSEF. Also, it was partially supported by the Manpower Development Program for Energy & Resources supported by the Ministry of Knowledge and Economy (MKE), Republic of Korea.

Appendix A. Derivation of the feasible range of m_3^P in the proposed three-zone SMB

In the derivation of this section, the superscript *P*, which stands for the proposed process, is omitted for the sake of simplicity. As mentioned in Section 2.3, the following two requirements should be satisfied in zone III for a successful separation in the proposed process (Fig. 2). First, the trailing edge of component B should exit zone III within a switching time. Secondly, the front of component A should be confined within zone III during the entire switching time.

The key idea for expressing the first requirement into a relevant equation lies in the migration path of the trailing edge of B, which stretches over zones I and III as delineated in the following. At the beginning of every switching period, the trailing edge of B is formed in zone I and then migrates some distance in zone I until the end of the switching period. As soon as the next switching period begins, the trailing edge of B is shifted from zone I to zone III, where it again migrates further distance until the end of the next switching period.

In order to meet the first requirement, it is obvious that the total migration distance of B in zones I and III during the aforementioned two consecutive switching periods must be larger than the single column length (L), which can be expressed by the following equation.

$$\left(\frac{\upsilon_1}{G_B}\right) t_{sw} + \left(\frac{\upsilon_3}{G_B}\right) t_{sw} > L \tag{A1}$$

where υ_j is the superficial velocity in zone j and $G_B \equiv \varepsilon_b + (1-\varepsilon_b)[\varepsilon_p + (1-\varepsilon_p)H_B]$. Multiplying both sides of the above equation by the cross-section area (S) and G_B, one can obtain

$$Q_1 t_{sw} + Q_3 t_{sw} > V_C\{\varepsilon_b + (1-\varepsilon_b)[\varepsilon_p + (1-\varepsilon_p)H_B]\} \tag{A2}$$

Using Eq. (2), the above equation can be re-expressed as follows.

$$m_1 V_C(1-\varepsilon) + V_C\varepsilon + m_3 V_C(1-\varepsilon) + V_C\varepsilon > V_C\{\varepsilon_b + (1-\varepsilon_b)[\varepsilon_p + (1-\varepsilon_p)H_B]\} \tag{A3}$$

Rearranging the above equation and using the relationships of $\varepsilon = \varepsilon_b + (1-\varepsilon_b)\varepsilon_p$ and $m_1 = m_{des}$, one can obtain

$$m_3 > H_B - \frac{\varepsilon}{1-\varepsilon} - m_{des} \tag{A4}$$

In addition, the mathematical expression relevant to the second requirement can be expressed as follows.

$$m_3 < H_A \tag{A5}$$

Combination of Eqs. (A4) and (A5) results in

$$H_B - \frac{\varepsilon}{1-\varepsilon} - m_{des} < m_3 < H_A \tag{A6}$$

References

[1] G.M. Zhong, G. Guiochon, Adv. Chromatogr. 39 (1998) 351.
[2] D.C.S. Azevedo, A.E. Rodrigues, AIChE J. 47 (2001) 2042.
[3] Y. Xie, B. Hritzko, C.Y. Chin, N.H.L. Wang, Ind. Eng. Chem. Res. 42 (2003) 4055.
[4] Y.-S. Bae, C.-H. Lee, J. Chromatogr. A 1122 (2006) 161.
[5] Y. Kawajiri, L.T. Biegler, AIChE J. 52 (2006) 1343.
[6] M. Minceva, P.S. Gomes, V. Meshko, A.E. Rodrigues, Chem. Eng. J. 140 (2008) 305.
[7] P.S. Gomes, A.E. Rodrigues, Chem. Eng. Technol. 35 (2012) 17.
[8] K.B. Lee, C.Y. Chin, Y. Xie, G.B. Cox, N.H.L. Wang, Ind. Eng. Chem. Res. 44 (2005) 3249.
[9] K.B. Lee, R.B. Kasat, G.B. Cox, N.H.L. Wang, AIChE J. 54 (2008) 2852.
[10] J.S. Hur, P.C. Wankat, Ind. Eng. Chem. Res. 44 (2005) 1906.
[11] R.C.R. Rodrigues, R.J.S. Silva, J.P.B. Mota, J. Chromatogr. A 1217 (2010) 3382.
[12] J.M.M. Araujo, R.C.R. Rodrigues, M.F.J. Eusebio, J.P.B. Mota, J. Chromatogr. A 1217 (2010) 5407.
[13] K. Hashimoto, M. Yamada, S. Adachi, Y. Shirai, J. Chem. Eng. Jpn. 22 (1989) 432.
[14] C.B. Ching, K.H. Chu, K. Hidajat, M.S. Uddin, AIChE J. 38 (1992) 1744.
[15] K.H. Chu, M.A. Hashim, Chem. Eng. J. 56 (1995) 59.
[16] Y. Zang, P.C. Wankat, Ind. Eng. Chem. Res. 41 (2002) 5283.
[17] Y.J. Jeon, M.B. Park, I.H. Kim, Bioprocess Biosyst. Eng. 33 (2010) 87.
[18] Y.A. Beste, W. Arlt, Chem. Eng. Technol. 25 (2002) 956.
[19] G. Paredes, S. Abel, M. Mazzotti, M. Morbidelli, J. Stadler, Ind. Eng. Chem. Res. 43 (2004) 6157.
[20] X. Wang, C.B. Ching, Chem. Eng. Sci. 60 (2005) 1337.
[21] S. Mun, J. Chromatogr. A 1218 (2011) 8060.
[22] A. Nicolaos, L. Muhr, P. Gotteland, R.M. Nicoud, M. Bailly, J. Chromatogr. A 908 (2001) 71.
[23] R. Wooley, Z. Ma, N.H.L. Wang, Ind. Eng. Chem. Res. 37 (1998) 3699.
[24] D.M. Ruthven, C.B. Ching, Chem. Eng. Sci. 44 (1989) 1011.
[25] G. Storti, M. Mazzotti, S. Carra, M. Morbidelli, Chem. Eng. Sci. 44 (1989) 1329.
[26] Z. Ma, N.H.L. Wang, AIChE J. 43 (1997) 2488.
[27] M.A. Cremasco, B.J. Hritzko, Y. Xie, N.H.L. Wang, Braz. J. Chem. Eng. 18 (2001) 181.
[28] S.F. Chung, C.Y. Wen, AIChE J. 14 (1968) 857.
[29] E.J. Wilson, C.J. Geankoplis, Ind. Eng. Chem. Fundam. 5 (1966) 9.
[30] R.B. Kasat, S.K. Gupta, Comput. Chem. Eng. 27 (2003) 1785.